

Polymer Communication

A new monomeric FRET-acceptor for polymer interdiffusion experiments on polymer dispersions

Andrey Turshatov, Jörg Adams*

Institute of Physical Chemistry, Clausthal University of Technology, Arnold-Sommerfeld-Strasse, 4, D-38678 Clausthal-Zellerfeld, Germany

Received 5 October 2007; accepted 17 October 2007

Available online 23 October 2007

Abstract

The properties of the non-fluorescent dye [1-(4-nitrophenyl)-2-pyrrolidinmethyl]-acrylate (NPP-A) have been evaluated with respect to its use in Fluorescence resonant energy transfer (FRET) experiments in polymers. NPP-A is attractive as a FRET-acceptor because its absorption spectrum has good spectral overlap with the emission spectrum of phenanthrene, where the latter is a widely used donor. Importantly, NPP does not fluoresce and therefore does not interfere with time-resolved measurements of the donor fluorescence. The label is well compatible with free radical polymerization. For two polymers, namely (butyl acrylate)-*co*-(methyl-methacrylate) (50/50) and (butyl methacrylate), the Förster radii were determined from the dependence of the FRET efficiency on the concentration of the acceptor. The results agree within the error. The Förster radius of the phenanthrene–NPP donor–acceptor pair was determined as $R_0 = 2.47 \pm 0.03$ nm.

© 2007 Elsevier Ltd. All rights reserved.

Keywords: Polymer dispersion; FRET; Interdiffusion

1. Introduction

Coatings based on waterborne polymer dispersion have numerous ecological and economical advantages compared to coatings prepared by evaporation of organic solvents. However, the process of film formation from aqueous dispersions entails certain complications and material constraints. In particular, a mechanically tough film is obtained only if the film undergoes an interdiffusion stage, termed “stage III” in the standard picture of film formation [1–3]. During stage III, polymer chains diffuse across the interparticle boundaries until the latter gradually disappear. Without interdiffusion, there is a lack of entanglement between polymer chains located on different spheres and the film easily fractures along the interparticle boundaries.

Interdiffusion can conveniently be probed with fluorescent resonant energy transfer (FRET) measurements. Briefly, one

employs a latex blend containing particles which are either labeled with donor groups or with acceptor groups. If donor and acceptor molecules approach each other within a distance of the Förster radius (typically a few nm), there is non-radiative energy transfer between the two, which modifies the fluorescence spectrum and the decay profile of the donor. FRET requires close proximity between donors and acceptors and is therefore only found if the two materials intermix. The Winnik group, in particular, has studied interdiffusion employing FRET under a large variety of conditions [4].

A widely used donor–acceptor pair for FRET is phenanthrene as the donor and anthracene as the acceptor [4a,5]. Phenanthrene is stable in free radical polymerization and has a low bleaching tendency. Its small size is also of advantage. In static fluorescence experiments, the fluorescence of either phenanthrene or anthracene is analyzed. Both, decrease of the donor fluorescence intensity and an increase of the acceptor fluorescence are indications for non-radiative energy transfer. While static measurements are simple, in principle, they are plagued by calibration problems. There are various artifacts, such as a drift of lamp intensity, time-dependent scattering

* Corresponding author. Tel.: +49 5323 72 3171; fax: +49 5323 72 2863.E-mail address: adams@pc.tu-clausthal.de (J. Adams).

phenomena, and drifts of the alignment. In time-resolved spectroscopy, one only observes the shape of the decay profile of the donor. FRET has a characteristic influence on the shape of the decay curve. When observing the donor fluorescence, one often has to employ a rather narrow band pass filter in order to cut the acceptor fluorescence, which would otherwise interfere with the measurement. For the analysis of thin films or for measurements with short acquisition times, a non-fluorescent acceptor is highly desirable, because a broader filter can be used, which increases the signal to noise ratio.

Winnik et al. have shown that non-fluorescent 4-(dimethylamino)-benzophenone derivatives can be used as acceptors for the study of interdiffusion processes [4c]. The phenanthrene/4-(dimethylamino)-benzophenone pair has Förster radius of $R_0 = 2.37$ nm, which is slightly higher than the Förster radius of the phenanthrene/anthracene pair ($R_0 = 2.3$ nm).

We report on the use of 4-nitrophenyl-2-pyrrolidinemethyl (NPP) and its polymerizable derivate [1-(4-nitrophenyl)-2-pyrrolidinemethyl]-acrylate (NPP-A) as non-fluorescing acceptors in conjunction with phenanthrene. Fig. 1 shows the chemical structure of NPP-A. To date, NPP mostly finds use in non-linear optics (NLO) materials [6,7]. The NPP-labeled monomer NPP-A is commercially available from Sigma-Aldrich. The absorption spectrum of NPP strongly overlaps with the emission spectrum of phenanthrene (Fig. 2a). The Förster radius depends on the spectral overlap via the relation

$$R_0^6 \propto \int_0^{\infty} F_D(\lambda) \varepsilon_A(\lambda) \lambda^4 d\lambda \quad (1)$$

Here $F_D(\lambda)$ is the donor fluorescence intensity and $\varepsilon_A(\lambda)$ is the extinction coefficient of the acceptor at that wavelength. Given the good overlap, one expects a large Förster radius of the phenanthrene–NPP pair. A high value of R_0 usually is of advantage because it allows for a small concentration of labels.

2. Materials and methods

The monomers butyl acrylate (BA), butyl methacrylate (BMA), methyl-methacrylate (MMA), and acrylic acid (AA) (Sigma-Aldrich) were distilled under reduced pressure directly before polymerization. The initiator AIBN (Sigma-Aldrich) was recrystallized from methanol. Sodium dodecylsulphate (SDS), hexadecane (HD), NPP-A (Sigma-Aldrich), and (9-phenanthryl)-methyl-methacrylate (Phe-MMA) (Toronto Research Chemicals) were used as received. Tetrahydrofuran (THF, Alfa Aesar, special grade) was used as the solvent for spectroscopic measurements.

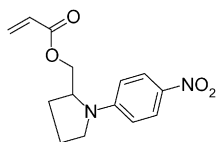


Fig. 1. Chemical structure of [1-(4-nitrophenyl)-2-pyrrolidinemethyl]-acrylate (NPP-A).

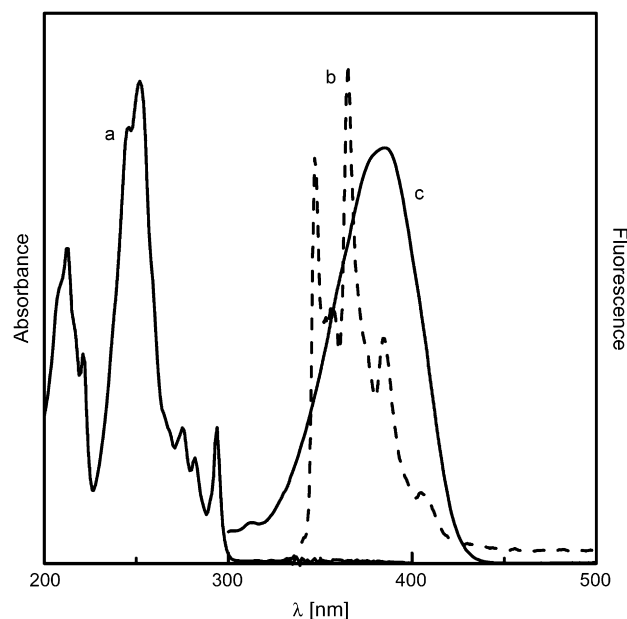


Fig. 2. Absorption and emission spectra of the dye-labeled polymer. (a): Absorption spectrum of the phenanthryl-labeled polymer **L1**; (b): emission spectrum of **L1**; (c): absorption spectrum of the NPP-labeled polymer **L2**. The extinction coefficient of **L2** at $\lambda_{\max} = 384$ nm was determined to be 18 333 l/mol cm.

2.1. Solution polymerization

AIBN (0.034 g) and Phe-MMA (0.0513 g,) (sample **S1**) or NPP-A (0.0108 g) (sample **S2**) were dissolved in 2 g of the MMA/BA (1/1) monomer mixture. To this were added 2.5 g of THF and the mixture was purged with nitrogen. Polymerization was carried out in a small vial for 20 h at 70 °C without stirring. The resulting polymer was precipitated into methanol and reprecipitated twice from THF solution into methanol. The concentration of NPP-A in the polymer was determined by UV–vis spectroscopy as 0.47 wt%.

2.2. Miniemulsion polymerization

Miniemulsion polymerization is better suited for the preparation of particles with defined chemical composition than conventional emulsion polymerization, because the ingredients do not have to diffuse through the aqueous phase in a particle growth phase. Thus, a better control of the product is reached. Water (16 g), MMA (1.98 g), BA (1.98 g), AA (0.04 g), SDS (0.048 g), HD (0.16 g), AIBN (0.068 g), and Phe-MMA (0.0712 g) (sample **L1**) or NPP-A (0.0421 g) (sample **L2**) were placed in a small vial. The mixture was purged with nitrogen for 30 min and then heated to 70 °C. The reaction was kept at this temperature for 20 h and then cooled to room temperature. The degree of conversion was determined gravimetrically to be between 98% and 99%.

Miniemulsion polymerization of BMA was carried out by the same way. Water (16 g), BMA (3.96 g), AA (0.04 g), SDS (0.048 g), HD (0.16 g), AIBN (0.068 g), and Phe-MMA (0.0712 g) (sample **L3**) or NPP-A (0.0421 g) (sample **L4**) were used.

2.3. Polymer characterization

Particle size distributions were determined by dynamic light scattering (DLS). The measurements were carried out at 25 °C on an ALV/DLS/SLS system equipped with a multi- τ digital correlator 5000E (ALV, Germany) at a scattering angle of 90°. A solid-state laser (ADLAS DPY 135, output power = 100 mW, $\lambda_0 = 632$ nm) was used as the light source. Size exclusion chromatography (SEC) in THF was used for the determination of the molecular weights. We used a UV and differential refractive index (DRI) detection, where the former is sensitive to the dye, while the latter is sensitive to the entire polymer. The columns (Styragel®, Waters) were calibrated against PMMA-standards. The glass temperature was measured by differential scanning calorimetry (DSC) using the DSC-7 instrument (Perkin Elmer) in a temperature range between –20 and 60 °C.

2.4. Spectroscopic measurements

Absorption and steady-state fluorescence spectra (Fig. 2) were acquired with a JASCO V550 UV–vis spectrophotometer and a SPEX Fluorolog 2 fluorescence spectrophotometer. Time-resolved measurements were carried out using time-correlated single-photon counting (TCSPC). Polymer films were prepared on a horizontal quartz plate. A light emitting diode (LED) with a center wavelength of 282 nm (PicoQuant, Germany) was used as the excitation source. Fluorescence photons were collected with light guide in reflection mode. A band pass filter ($\lambda = 325$ –480 nm) and a photomultiplier tube (Hamamatsu 1P28) were used to select and detect the photons. The signals were processed with a modular electronics setup (ORTEC EG&G). All experiments were carried out at 25 °C in ambient

humidity. A few reference experiments under nitrogen atmosphere gave the same results as the experiments in air.

2.5. Data analysis in TCSPC experiments

The fluorescence intensity decays were fitted with the function

$$I(t) = A \exp\left(-\frac{t}{\tau_D} - 2\gamma\sqrt{\frac{t}{\tau_D}}\right) \quad (2)$$

using a non-linear least square fit routine including forward folding of the fit function with the instrument function. The parameter A is a prefactor. The intrinsic lifetime of the donor fluorescence, τ_D , was determined as $\tau_D = 44.3$ ns (BA-MMA matrix) and 44.7 ns (BMA matrix) in the absence of the acceptor ($\gamma \equiv 0$) and maintained fixed at this value when fitting decays with a non-zero γ . The FRET efficiency is contained in the parameter γ . Under conditions of a spatially uniform acceptor concentration, C_A (in units of mol/L), one has

$$\gamma = \frac{C_A}{A_0} = \frac{2\pi^{3/2}N_A R_0^3 C_A}{3000} \quad (3)$$

where A_0 is a critical acceptor concentration, N_A is Avogadro's number, and R_0 is the Förster radius in units of centimeter. At the critical concentration, A_0 , the mean distance between donor and acceptor moieties is about equal to the Förster radius. Eq. (3) is used below to calculate the Förster radius.

3. Results

Successful incorporation of the new NPP label into the polymer chain is proven by SEC. Fig. 3 shows the SEC traces

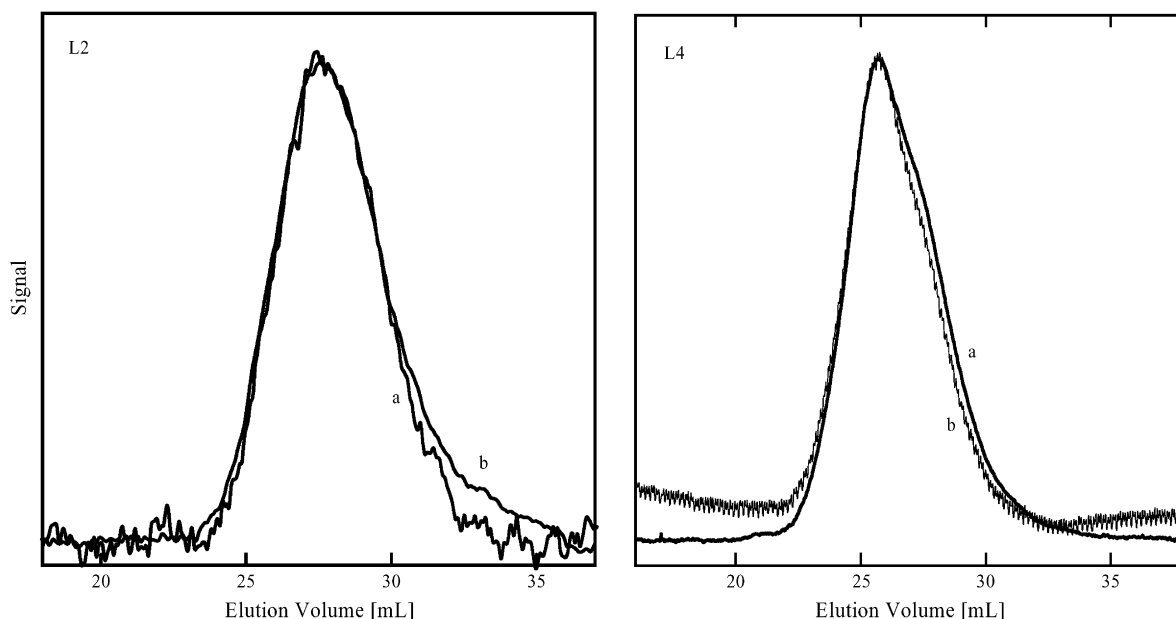


Fig. 3. Size exclusion chromatography (SEC) traces of polymer **L2** and **L4** in THF at a concentration of 1 mg/mL. (a): Signal from the UV detector at 354 nm; (b): signal from the differential refractive index (DRI) detector. The two detectors are sensitive to the dye and to the entire polymer, respectively. The two signals overlap, indicative of uniform incorporation of the label.

Table 1
Material properties

Sample	Radius [nm]	M_w [kg/mol]	M_w/M_n	T_g [°C]
S1		22.4	2.4	20
S2		30.4	1.6	20
L1	55	16.7	3.6	24
L2	65	11.6	4.2	23
L3	46	181.8	6.45	19
L4	49	94.7	3.8	19

of the polymers **L2** and **L4** detected with a UV detector (which is sensitive to the NPP unit) and by a DRI detector (which is sensitive to the entire polymer). The two signals overlap, indicating that the label reacts uniformly during the polymerization. We did not observe excess of label for low or high molecular weight fractions. Table 1 shows material parameters of the polymers. The particle sizes of the phenanthryl-labeled polymer (**L1**, **L3**; $r = 55$ and 46 nm) and the NPP-labeled polymer (**L2**, **L4**; $r = 49$ and 65 nm) are similar.

Quantitative analysis of interdiffusion measurements requires knowledge of the Förster radius. Mixtures of phenanthryl-labeled polymer with NPP-labeled polymer with various acceptor concentrations were prepared in THF solution. Thin, dry films were cast onto glass substrates. The decay profiles of the donor fluorescence (Fig. 4) have the characteristic shape for FRET. Fig. 5 shows the parameter 2γ versus the acceptor concentration C_A , for the polymers prepared in solution (**S1/S2**) and, the polymers prepared as miniemulsions (**L1/L2** and **L3/L4**). From the slope in the 2γ vs. C_A plot, one derives the Förster radius according to Eq. (3). We obtain values of $R_0 = 2.45$ and 2.50 nm for the copolymers prepared from THF solution and the miniemulsion, respectively. For the BMA, we find $R_0 = 2.47$ nm. They are higher than the

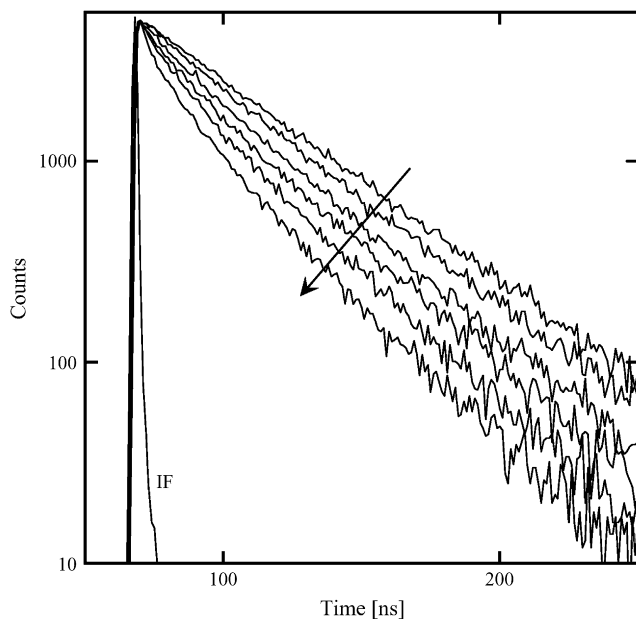


Fig. 4. Decay profiles of the phenanthryl fluorescence of polymer **L1** mixed with the NPP-labeled polymer **L2**. The arrow indicates increasing acceptor (NPP-A) concentration.

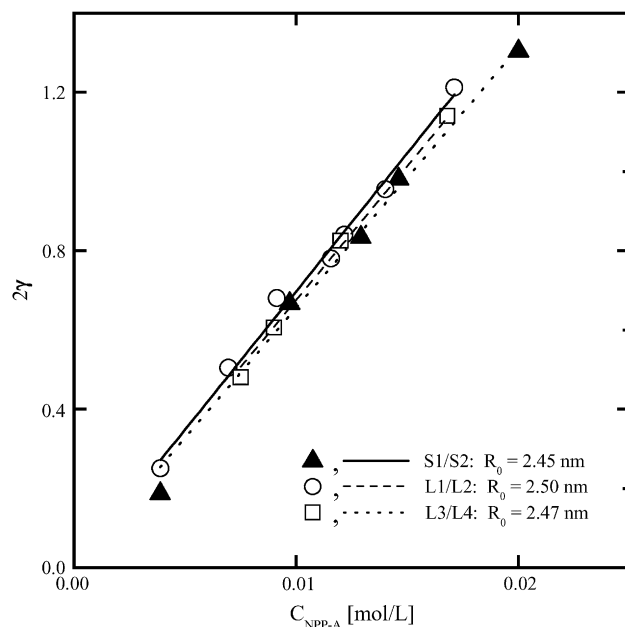


Fig. 5. Coefficient 2γ as a function of the NPP-A concentration. The Förster radius is derived from the slope by means of Eq. (3). Solid triangles – mixture of **S1** and **S2**, which are polymers prepared in solution, open circles – mixture of **L1** and **L2**, open squares – mixture of **L3** and **L4**. The lines are linear fits through the origin.

Förster radii of the phenanthrene/anthracene pair (2.3 nm) and the phenanthrene/4-(dimethylamino) benzophenone pair (2.37 nm). The increased R_0 allows to reduce the acceptor concentration by more than 20% relative to the phenanthrene/anthracene pair while maintaining the same amount of energy-transfer constant.

In the following we address the issue of homogeneity. Eq. (3) assumes that both the donor and the acceptor are statistically distributed in space. Deviations from such an ideal situation may come about in different ways. For the BA/MMA copolymers, the sample may have fluctuating concentrations of BA and MMA because the copolymerization parameters of these two monomers differ [8]. If polymer chains produced in an early and in a late stage of the polymerization process differ in their MMA content, the MMA-rich chains might be preferentially located close to each other. Fluctuations in MMA concentration (and in dye concentration, as a consequence) may result. While BA-co-MMA is a system of high practical relevance, it is not optimal for the determination of R_0 . For dye-labeled BMA polymer, the situation is improved, but there is still the possibility that the copolymerization parameters of the dyes and BMA differ. Since the dye is highly diluted, the composition fluctuations are smaller in this case. Also, since the molecular weight usually increases with conversion due to the gel effect, one would expect a correlation between dye concentration and molecular weight. Such a correlation if present, is very small, as evidenced from the SEC traces (Fig. 3). Finally, the fact that all the three samples yielded a similar value of R_0 lends credibility to this result. While, admittedly, an ideally statistical dye

distribution is not guaranteed, its effect on the derived values of R_0 should be small.

4. Conclusions

The acrylic monomer [1-(4-nitrophenyl)-2-pyrrolidin-methyl]-acrylate (NPP-A) was co-polymerized with different acrylic monomers in solution and in miniemulsion. The dye molecule is a suitable acceptor in FRET experiments. The phenanthrene–NPP pair exhibits a high Förster radius of $R_0 = 2.47 \pm 0.03$ nm. Because NPP is non-fluorescent, the FRET experiments can be carried out employing a broad band pass filter or an edge filter (only removing scattered light). This entails a substantial improvement in sensitivity, compared to fluorescent acceptors.

Acknowledgement

This work was funded by the EU under contract IP 011844-2 (NAPOLEON).

References

- [1] Keddie JL. Mater Sci Eng 1997;R21:101.
- [2] Winnik MA. Curr Opin Colloid Interface Sci 1997;2:192.
- [3] Steward PA, Heran J, Wilkinson MC. Adv Colloid Interface Sci 2000; 86:195.
- [4] (a) Zhao CL, Wang Y, Hruska Z, Winnik MA. Macromolecules 1990; 23:4082;
(b) Feng J, Pham H, Stoeva V, Winnik MA. J Polym Sci Part B Polym Phys 1997;36:1129;
(c) Ye X, Farinha JPS, Oh JK, Winnik MA, Wu C. Macromolecules 2003;36:8749;
(d) Wu J, Winnik MA, Farwaha R, Rademacher J. Macromol Chem Phys 2003;204:1933;
(e) Oh JK, Yang J, Rademacher J, Farwaha R, Winnik MA. Macromolecules 2004;37:5752.
- [5] Baumgart T, Cramer S, Jahr T, Veniaminov A, Adams J, Fuhrmann J, et al. Macromol Symp 2000;151:451.
- [6] Yoshida M, Asano M, Tamada M, Kumakura M. Makromol Chem Rapid Commun 1989;10:517.
- [7] Feng Z, Wang J, Wang Y, Ye C. Synth Met 1993;57:3945.
- [8] Brandrup J, Immergut EH, Grulke EA. Polymer handbook, vol. II. John Wiley & Sons; 1999. p. 228.